Proc. Natl. Acad. Sci. USA
Vol. 88, pp. 7500–7504, September 1991
Cell Biology

cAMP-inducible chloride conductance in mouse fibroblast lines stably expressing the human cystic fibrosis transmembrane conductance regulator

(full-length cDNA/chloride channel/cAMP regulation)

JOHANNA M. ROMMENS*, SASCHA DHO†, CHRISTINE E. BEAR†‡, NORBERT KARTNER§, DARA KENNEDY*, JOHN R. RIORDAN§¶, LAP-CHEE TSUI*‖, AND J. KEVIN FOSKETT†

*Department of Genetics, †Division of Cell Biology, and §Department of Biochemistry, Research Institute, The Hospital for Sick Children, Toronto, ON M5G 1X8, Canada; and Departments of ‡Physiology, ¶Biochemistry and Clinical Biochemistry, and ‖Molecular and Medical Genetics, University of Toronto, Toronto, ON M5S 1A8, Canada

Communicated by Robert W. Berliner, May 15, 1991

ABSTRACT **A cAMP-inducible chloride permeability has been detected in mouse fibroblast (L cell) lines upon stable integration of a full-length cDNA encoding the human cystic fibrosis transmembrane conductance regulator (CFTR). As indicated by a Cl^--indicator dye, the Cl^- permeability of the plasma membrane increases by 10- to 30-fold within 2 min after treatment of the cells with forskolin, an activator of adenylyl cyclase. The properties of the conductance are similar to those described in secretory epithelial cells; the whole-cell current–voltage relationship is linear and there is no evidence of voltage-dependent inactivation or activation. In contrast, this cAMP-dependent Cl^- flux is undetectable in the untransfected cells or cells harboring defective cDNA constructs, including one with a phenylalanine deletion at amino acid position 508 (ΔF508), the most common mutation causing cystic fibrosis. These observations are consistent with the hypothesis that the CFTR is a cAMP-dependent Cl^- channel. The availability of a heterologous (nonepithelial) cell type expressing the CFTR offers an excellent system to understand the basic mechanisms underlying this CFTR-associated ion permeability and to study the structure and function of the CFTR.**

Cystic fibrosis (CF) is the most common autosomal recessive disease in the Caucasian population (1). The recent identification of the gene (2–4) and mutations (4–9) responsible for CF has provided insight into the basic defect in this disease. The protein product of this gene has an estimated molecular mass of 170 kDa with transmembrane and nucleotide-binding-fold domains. It has structural similarity to proteins with known transport functions (3, 10).

The development of assay systems to study the function of the CF transmembrane conductance regulator (CFTR) has been hampered by the inability to reconstruct a full-length CFTR cDNA by ligation of cloned fragments. Most of the resulting constructs appeared to be unstable in *Escherichia coli*, probably due to a sequence in the exon 6b region that resembles a prokaryotic promoter element (11, 12). The use of a low-copy-number plasmid vector can apparently overcome this difficulty (11). We have altered the DNA sequence in exon 6b and also obtained a stable construct (12).

Two studies (12, 13) show that, upon transfection of a full-length cDNA construct into epithelial cells derived from CF patients, a deficient cAMP-dependent Cl^- conductance can be restored. In addition, expression of exogenous CFTR has been correlated with the appearance of cAMP-regulated Cl^- conductance in nonepithelial cells (14, 15), where such activity is normally absent, consistent with the hypothesis that CFTR can function as a Cl^- channel itself (3).

In this communication, we describe the construction and use of a mammalian expression vector to produce human CFTR in a long-term mouse fibroblast culture. We show that expression of CFTR induces a cAMP-dependent Cl^- conductance, which is normally not observed in these cells. This expression system may be suitable for study of the Cl^- conductance pathway and its regulation and to understand the structure and function of CFTR.

MATERIALS AND METHODS

Plasmid Vectors. The mammalian expression vector pCOF-1 is a derivative of pSGM3X, which is similar to pSGM1 (16), except that the human metallothionein IIa promoter (17) was inserted in the opposite orientation and a *Xho* I site was inserted in the *Kpn* I site within the *Ecogpt* gene. To reconstruct the full-length CFTR cDNA in pCOF-1 (Fig. 1), the bulk of the coding region (exons 2–24) was obtained from partial cDNA clones (3), except that three silent nucleotide substitutions (T → C at position 930, A → G at position 933, and T → C at position 936) were introduced into the exon 6b region with oligonucleotide-mediated mutagenesis by the polymerase chain reaction (19, 20). The 3′ untranslated region of CFTR in pCOF-1 was derived from the genomic DNA clone TE27E2.3 (2). The entire coding region of exon 1 (from the initiation codon to the *Pvu* II site) was generated by two complementary synthetic oligonucleotides and the Klenow fragment of DNA polymerase I, where a single nucleotide substitution (C → G) was introduced immediately after the initiation codon (underlined in the legend to Fig. 1) to create a *Nco* I site for ligation to the human metallothionein IIa promoter. The latter substitution changed the encoded amino acid from glutamine to glutamic acid. The construction of control plasmid pCONZ was similar to that of pCOF-1, except that a single nucleotide was deleted 35 base pairs downstream from the initiation codon. A truncated protein would be predicted from this frameshift construct. The plasmid pCOFΔF508 was generated by replacing sequences of exons 9–13 in pCOF-1 with the corresponding fragment from C1-1/5, a cDNA containing the ΔF508 mutation. The full-length cDNA clone pBQ6.2 contained a 6.2-kb *Pst* I fragment in pBluescript (Stratagene) and was constructed similarly to pCOF-1 except that the exon 1 region was derived from clone 10-1. The integrity of the CFTR cDNA inserts in pBQ6.2 and pCOF-1 and the critical regions in the other plasmid constructs were verified by DNA se-

The publication costs of this article were defrayed in part by page charge payment. This article must therefore be hereby marked "*advertisement*" in accordance with 18 U.S.C. §1734 solely to indicate this fact.

Abbreviations: CF, cystic fibrosis; CFTR, CF transmembrane conductance regulator; SPQ, 6-methoxy-1-(3-sulfonatopropyl)quinolinium.

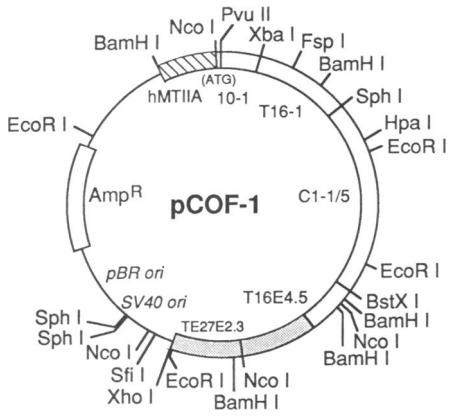

FIG. 1. Expression vector pCOF-1. The complete CFTR coding region (open boxes) is positioned downstream from the human metallothionein IIa (hMTIIa) promoter (hatched box). The human metallothionein IIa initiation codon is joined with that of CFTR at an *Nco* I site introduced by the synthetic oligonucleotides 5′-CACTGCAGACCATGGAGAGGTCGCCTCTGGAAAAGGC-CAGCGTT-3′ and 5′-GACTGCAGCTGAAAAAAAGTTTG-GAGACAACGCTGGCCTT-3′, as described in the text. The DNA sequence from exon 2 to 24 and its 3′ flanking region was derived from clones 10-1 (*Pvu* II–*Xba* I), T16-1 (*Xba* I–*Sph* I), C1-1/5 (*Sph* I–*Bst*XI), T16E4.5 (*Bst*XI–*Nco* I), and TE27E2.3 (*Nco* I–*Xho* I), as indicated. In pCOFΔF508, the 1-kilobase (kb) *Bam*HI–*Hpa* I fragment was replaced with the corresponding fragment from clone C1-1/5.

quencing. (Detailed construction procedures are available from J.M.R. on request.) The plasmid vector (pSTK7) containing the herpes simplex virus thymidine kinase gene, used in the cotransfection experiments, has been described (16). Bacterial cell cultures and plasmid DNA samples were prepared according to standard procedures (18).

Cell Culture and DNA Transfection. Each of the three test plasmids (20 μg), pCOF-1, pCONZ, and pCOFΔF508, was cotransfected with pSTK7 (1 μg) into mouse LTK$^-$ cells by calcium phosphate coprecipitation (16). Biochemical selection for thymidine kinase-positive cells was achieved in minimal essential medium supplemented with hypoxanthine/aminopterin/thymidine (HAT; GIBCO/BRL). In some experiments, the test plasmids were linearized at the unique *Sfi* I site (Fig. 1). High molecular weight DNA was isolated from each clonal cell line (21), digested with restriction enzymes *Eco*RI, *Bam*HI, and *Nco* I, and analyzed by agarose-gel-blot hybridization (18) with the full-length cDNA (insert from pBQ6.2) as probe. Total RNA was extracted (22) and analyzed by agarose-gel-blot hybridization (18).

Protein Analysis. Cells were homogenized in a hypotonic buffer containing 10 mM KCl, 1.5 mM $MgCl_2$, and 10 mM Tris·HCl (pH 7.4). Nuclei and mitochondria were collected by centrifugation at 4000 × *g* for 5 min (fraction A). A crude light membrane fraction was then collected by centrifugation at 9000 × *g* for 15 min (fraction B). Membrane pellets were dissolved in loading buffer and separated on a $NaDodSO_4$/polyacrylamide (6%) gel (23). Proteins were transferred to nitrocellulose as described (24) and immunodetected with monoclonal antibody M3A7 (14).

6-Methoxy-1-(3-sulfonatopropyl)quinolinium (SPQ) Fluorescence Assay. L cells grown on glass coverslips for 1–2 days were uniformly loaded with the Cl$^-$-indicator dye SPQ (Molecular Probes) by incubation in hypotonic (1:2 dilution) medium containing 20 mM SPQ at room temperature for 4 min. The mounted coverslip was perfused continuously at room temperature with medium containing 138 mM NaCl, 2.4 mM K_2HPO_4, 0.8 mM KH_2PO_4, 10 mM Hepes, 1 mM $CaCl_2$, 10 mM glucose, and 10 μM bumetanide (pH 7.4) on the stage of an inverted microscope. NO_3^- medium was identical except that NO_3^- replaced all but 10 mM Cl$^-$. To minimize Cl$^-$ fluxes through nonconductive pathways, we performed the experiments in the absence of HCO_3^- and in the presence of bumetanide, inhibiting the anion exchanger and Cl$^-$/cation cotransporters, respectively. Fluorescence and differential interference contrast imaging were performed simultaneously (25–27). SPQ fluorescence intensities (*F*) were normalized to total SPQ fluorescence F_0, determined as *F* measured in the absence of intracellular Cl$^-$, since autofluorescence was negligible. Calibrations (n = 7 cells) were performed essentially as described (27). The effective quenching constant K_{Cl} was 15 M^{-1}; the resting intracellular Cl$^-$ concentration was ≈70 mM. Cell volume changes were obtained by planimetry of differential interference contrast images (26, 27) and are presented as relative changes in the areas of the measured optical sections. By exposure of the cells to media of various osmolarities, we observed that differential interference contrast imaging of a single optical section can detect volume changes (not shown).

Whole-Cell Current Recordings. Membrane currents were measured at room temperature 12–24 hr after plating cells with whole-cell patch-clamp techniques (28). The patch pipet contained 110 mM sodium gluconate, 25 mM NaCl, 8 mM $MgCl_2$, 10 mM Hepes, 4 mM Na_2ATP, and 5 mM Na_2EGTA (pH 7.2). The bath contained 135 mM NaCl, 2.4 mM K_2HPO_4, 0.8 mM KH_2PO_4, 3 mM $MgCl_2$, 1 mM $CaCl_2$, 10 mM Hepes, and 10 mM glucose (pH 7.2). To examine the time course of cAMP-evoked conductance changes, membrane potentials were alternately clamped at −30 and +20 mV for 600 and 400 ms, respectively. Current–voltage relationships were determined by measuring the currents at the end of 400-ms voltage steps from 0 mV to ±70 mV (10-mV increments). Cell capacitance was compensated using cancellation circuitry of the EPC7 patch-clamp amplifier.

RESULTS

DNA Transfection. Stable mouse fibroblast cell lines containing full-length CFTR or mutant cDNA, as well as cell lines with the pSTK7 plasmid alone, were established. Four cell lines with pCOF-1 (4a-2C, 4a-3I, 4a-3K, and 4a-4S) contained an intact human metallothionein IIa promoter and the CFTR coding region, as judged by DNA analysis (data not shown). Similarly, four cell lines (6a-1D, 6a-2F, 6b-I, and 6b-K) for pCONZ (the control cDNA with the frame-shift mutation), three (5-2C, 5-1A, and 5-2D) for pCOFΔF508 (the cDNA with the major CF mutation), and two for pSTK7 (2a-4A and 2a-3C) were identified.

RNA Analysis. Abundant levels of RNA transcripts of ≈10 kb in size were detected in cDNA transfected cells (Fig. 2*A*). Although their size was larger than the anticipated 6.2 kb, the result appeared to be consistent among all cell lines. It seemed probable that an alternative polyadenylylation site(s) instead of those contained in the cDNA constructs were utilized. Thymidine kinase-specific transcripts were detected in all HAT-resistant cell lines tested (data not shown).

Protein Analysis. Cells expressing CFTR mRNA (as represented by the cell line 4a-3I) contained an antibody-reacting protein band that was indistinguishable from mature CFTR expressed endogenously in membranes of the colonic carcinoma cell line T-84 (Fig. 2*B*). The amount of protein was within the range of that observed for T84 cells, with a significant portion in the light membrane fraction. Reacting bands were not detected in untransfected LTK$^-$ cells or in cells transfected with a CFTR gene predicted to produce a truncated product (line 6B-I). The latter result was expected as the antibody was directed against the C terminus of the protein. No immunoreactive material was observed for CFTRΔF508 in the examined fractions (line 5-2D) (29). It was therefore uncertain if the mutated protein was produced in these transfected cells.

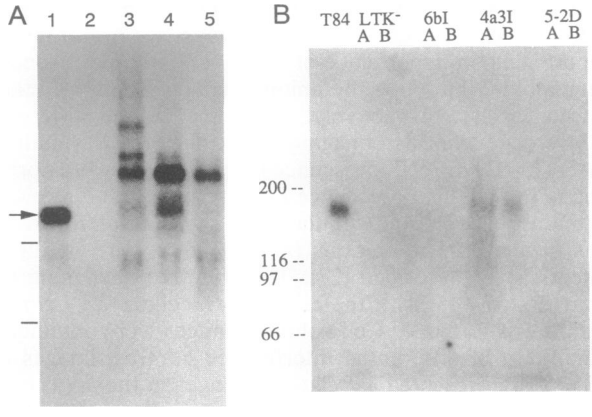

FIG. 2. RNA and protein analysis of mouse L cell lines expressing human CFTR. (*A*) Total RNA from Caco2 (5 μg, lane 1), LTK⁻ (10 μg, lane 2), 6B-I (10 μg, lane 3), 4a-3I (10 μg, lane 4), and 5-2D (10 μg, lane 5) cell lines was electrophoresed on a 1% formaldehyde/agarose gel, transferred to Hybond-N (Amersham), and hybridized with ^{32}P-labeled cDNA probe. The 6.2-kb CFTR mRNA of the Caco2 cell line is indicated with the arrow. The relative positions of the 28S and 18S rRNAs are indicated by tick marks. (*B*) Protein fractions from nuclei and mitochondria (lanes A) and crude light membranes (lanes B) from the cell lines T84, LTK⁻, 6B-I, 4a-3I, and 5-2D. Bands were visualized by ^{125}I-labeled rabbit anti-mouse antibody. Molecular masses in kDa are indicated.

SPQ Fluorescence Assay. To investigate if expression of CFTR affected a Cl^- conductance, a single-cell assay based on quantitative fluorescence intensity measurements of the Cl^- indicator dye SPQ was performed. The basic protocol involved exposing cells to NO_3^- medium followed by return to normal Cl^- medium. Since NO_3^- is generally permeable through Cl^- channels but, unlike Cl^-, does not quench SPQ, changes in SPQ fluorescence intensities due to these anion substitutions measure unidirectional Cl^- fluxes; the rate of change measures cell Cl^- permeability. Forskolin (10 μM) was added subsequently to increase intracellular levels of cAMP. After a 2-min exposure to forskolin, the medium was again switched to the NO_3^- medium, in the continued presence of forskolin. Thus each cell was used as its own control to evaluate the Cl^- permeability induced by cAMP.

Only slow changes in SPQ fluorescence intensity were observed in cells with the frame-shift CFTR construct (as represented by line 6B-I) upon exposure to NO_3^- medium (Fig. 3*A*), indicating that these cells maintained a low resting Cl^- permeability. Exposure of these transfected control cells to forskolin did not have any effect (n = 41 cells from four passages). Similar results were obtained from cells transfected with the thymidine kinase gene only (line 2a-4A, n = 22 cells) and from untransfected cells (n = 18 cells) (data not shown).

Exposure of cells expressing CFTR to NO_3^- medium similarly elicited little or no change in SPQ fluorescence intensity (as represented by line 4a-3I in Fig. 3*C*), indicating that CFTR expression *per se* did not enhance Cl^- permeability. In contrast, a second exposure to NO_3^-, during forskolin stimulation, caused a rapid loss of intracellular Cl^- (Fig. 3*C*). This response was highly reproducible: there was a 20- to 30-fold increase of unidirectional Cl^- flux (30) from ≈0.03 mM/s to 0.9 mM/s, for each of the 10 cells in the microscopic field (Fig. 3*C*). Of 106 cells examined from eight passages, all responded similarly. Similar results were obtained from another cell line expressing CFTR (clone 4a-3K, n = 23 cells). In the continued presence of forskolin (Fig. 3*D*), Cl^- permeability remained enhanced at near maximal levels for as long as 30 min, the extent of our measurements (n = 12 cells).

There were no volume changes during exposure of forskolin-stimulated CFTR cells to NO_3^- (data not shown), indicating that the substantial changes in the intracellular concentration of Cl^- were not associated with changes in cell salt content. Therefore, the Cl^- fluxes were likely to be associated with equal fluxes of NO_3^- in the opposite direction. The lack of changes in intracellular Cl^- concentration or cell volume during forskolin stimulation in Cl^- medium demonstrates that neither CFTR expression nor cAMP conferred enhanced cation conductance. Together with the enhanced Cl^- permeability, cell shrinkage or swelling would have been observed if there were a high K^+ conductance or high Na^+ conductance, respectively.

Cl^- permeability was also examined in cells containing a CFTRΔF508 construct. These cells (as represented by clone 5-2D, n = 15 cells) exhibited low Cl^- permeability under resting conditions, and the permeability could not be enhanced by forskolin (Fig. 3*B*).

To establish that the cAMP-induced Cl^- permeability in the CFTR-expressing cells was due to activation of a Cl^- conductance, gramicidin was included in the normal Cl^- medium to increase cation conductance of the plasma membrane. Under these conditions, the presence of a Cl^- channel would result in a substantial influx of both Na^+ and Cl^-, causing extensive cell swelling. Exposure to gramicidin had no effect on SPQ fluorescence or cell volume in cells with the frame-shift CFTR construct (n = 13 cells) or an intact CFTR construct (n = 33 cells) (Fig. 3*E*), supporting our conclusion (above) that resting Cl^- conductance was negligible in both the control and CFTR cells. After the addition of forskolin, however, there was a marked rapid cell swelling, after a lag period of from 30 to 90 s, accompanied by elevated intracellular Cl^- concentration in the cells expressing CFTR but not in control cells (Fig. 3*E*). These results demonstrated that the basis of cAMP-induced Cl^- permeability observed in CFTR-expressing cells was a Cl^- channel.

cAMP-Stimulated Cl^- Currents in CFTR-Expressing Cells. Corroborating the results of the fluorescence assay, whole-cell current was stimulated in cells expressing CFTR (Fig. 4*A*). After a lag period of ≈30 s, outward current in 11 of 11 cells increased dramatically to a plateau, which was sustained for 2–5 min before decreasing toward control values. This "run down" contrasts with findings using the SPQ assay, possibly reflecting a depletion of cytosolic factors necessary for sustained activation in the whole-cell patch-clamp configuration. Currents evoked by the activation cocktail did not display any time-dependent voltage effects (Fig. 4*B*). In contrast to the expressing cells, none of the 9 cells containing the frame-shift CFTR construct exhibited a response to the activation cocktail (Fig. 4*A*).

Current–voltage relations were essentially linear in both cells transfected with the intact CFTR and the frame-shift CFTR constructs (not shown). Slope conductances of 1.8 ± 0.4 nS and 1.9 ± 0.5 nS (n = 9) were calculated in control cells before and after treatment with the activation mixture, respectively. The slope conductance in CFTR-expressing cells was similar (1.6 ± 0.1 nS) but treatment with the activation mixture induced an ≈13-fold increase to 20.1 ± 1.7 nS (n = 10) (Fig. 4*C*).

The reversal potential of the cAMP-activated current in cells expressing CFTR was −17 ± 5 mV, approaching the equilibrium potential for Cl^- under standard conditions (E_{Cl} = −32 mV). From this measurement, the calculated anion versus cation permeability was ≈5:1. Anion selectivity was assessed in cAMP-activated cells by replacing bath NaCl (135 mM) with sodium gluconate (135 mM). This manipulation resulted in a shift in reversal potential to +33 ± 8 mV (n = 4), toward the predicted E_{Cl} of +41 mV (Fig. 4*C*).

DISCUSSION

For this study, a general mammalian expression vector was constructed that is capable of directing the expression of CFTR cDNA in heterologous cell types. Three nucleotide

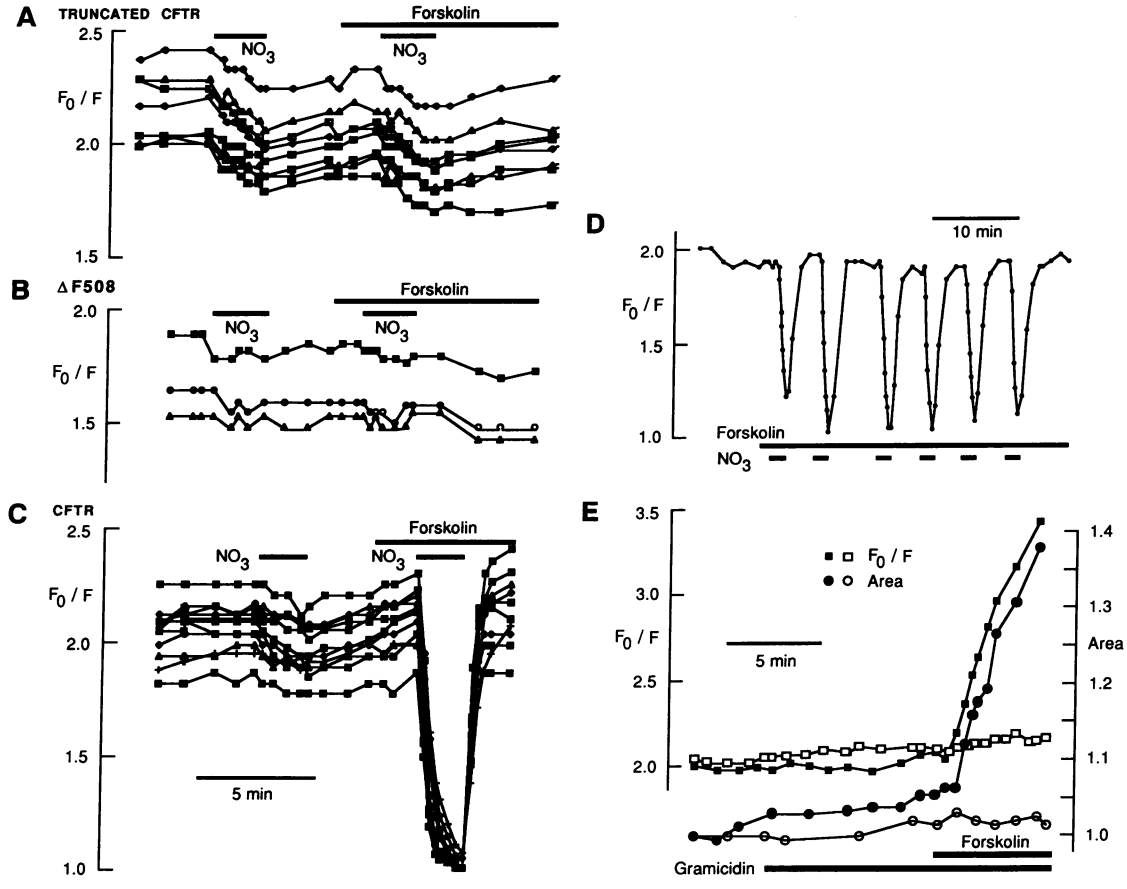

FIG. 3. Video microscopic detection of Cl^- permeability in single L cells. SPQ fluorescence intensities (F) are expressed relative to SPQ fluorescence intensity in the absence of Cl^- quenching (F_0); the direction of changes in F_0/F reflect parallel changes in intracellular Cl^- concentration. (*A–C*) Single cells, each indicated by a different symbol, are shown containing a frameshift construct leading to a predicted truncated CFTR (*A*); a mutant construct, CFTRΔF508 (*B*); and an intact construct, CFTR (*C*). Forskolin (10 μM) and NO_3^- medium were perfused over the cells for the periods indicated by solid bars. Time scale in *C* applies to *A–C*. (*D*) A single CFTR cell was repeatedly pulsed with NO_3^- medium. Rate of fluorescence change as well as peak response during constant pulses (1 min) was unchanged over the time course of exposure to forskolin, indicating that the cAMP-induced Cl^- permeability is sustained. (*E*) Simultaneous determinations of Cl^- concentration (F_0/F) (open and solid squares) and cell volume, expressed as relative area of a constant optical section (open and solid circles), in a single cell expressing CFTR (solid squares and circles) and a single cell expressing truncated CFTR (open squares and circles). As indicated, the cells were exposed to 5 μM gramicidin and to 10 μM forskolin.

substitutions were introduced in the coding region to disrupt the DNA sequence that appeared to cause instability of the full-length cDNA in bacterial hosts. The encoded amino acids were not altered with these changes.

The stable CFTR-expression system described in this study offers an attractive assay system to study the function of CFTR and complements the methods based on retrovirus (12), vaccinia virus (13), and baculovirus (14). (*i*) Similar

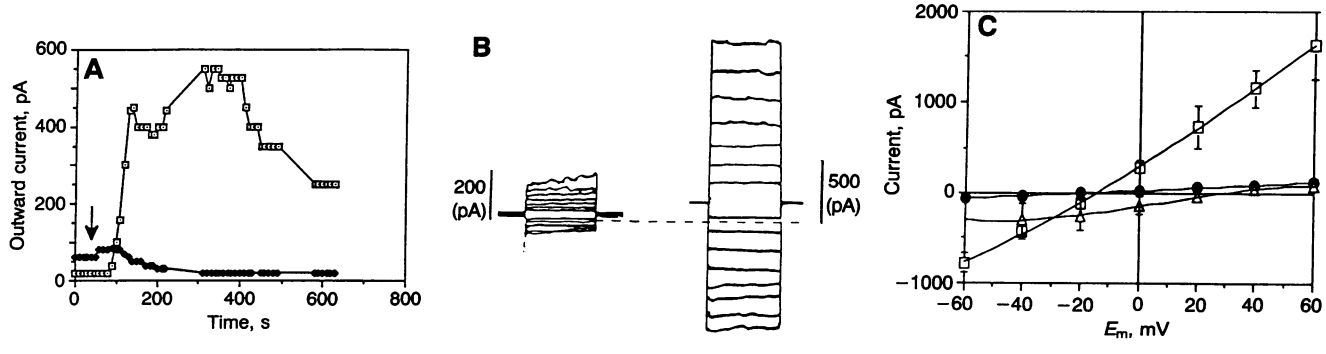

FIG. 4. Whole-cell Cl^- currents in transfected L cells. (*A*) Time course of whole-cell currents measured from cells transfected with the frame-shift CFTR (control) construct (solid diamonds) and the intact CFTR construct (open squares) after the addition of a solution containing 10 μM forskolin, 1 mM isobutylmethylxanthine, and 100 μM $N^6,O^{2'}$-dibutyryladenosine 3′,5′-cyclic monophosphate. The arrow indicates the time of solution addition. Outward currents were measured at $E_m = +20$ mV. (*B*) Whole cell current–voltage relationships for a CFTR-expressing cell before (*Left*) and 3 min after (*Right*) induced activation. The current scale for the nonstimulated cells is shown enlarged as indicated. The dashed line indicates the zero-current level. (*C*) Mean current–voltage relationships for CFTR cells ($n = 10$) before and after activation (solid circles and open squares, respectively). Replacement of bath NaCl with sodium gluconate resulted in a shift in reversal potential of cAMP-activated currents (open triangles) ($n = 4$).

optical and electrophysiological results have been obtained for a large number of transfected cells from various passages, indicating that expression of CFTR from the integrated cDNA is stable and cell cycle independent. In contrast, the conductance response seems to be rather heterogenous for virus-infected cells (13, 15).

(*ii*) The basal level of Cl^- conductance in the CFTR-expressing mouse L cells appears to be relatively low in comparison to that observed in the transiently transfected Sf9 insect cells (14), airway epithelial cells (13), CHO cells, HeLa cells, or mouse 3T3 fibroblasts (15). The remarkable Cl^- conductance increase observed upon cAMP stimulation (up to 30-fold) may present a unique opportunity to determine relative degrees of function to understand the varied phenotypes observed for CF patients with various genotypes.

(*iii*) Although L cells are of fibroblast origin, the cAMP-inducible Cl^- conductance in the CFTR-expressing cells appears to be the same as that detected in epithelial cells. The current–voltage relationship of the activated current is linear (31); there is no evidence of voltage-dependent current inactivation or activation; the magnitude of the cAMP-mediated Cl^- permeability is large. Further, there is a lag of 30–60 s preceding the enhancement of Cl^- conductance by forskolin, typical of whole-cell current measured in epithelial cells (31). A 5- to 10-pS Cl^- channel with linear current–voltage relationship is activated by cAMP in several types of epithelial cells, including the colonic cell lines T-84 (32) and Caco2 (C.E.B. and E. F. Reyes, unpublished observations) as well as pancreatic duct cells (33). It is likely that the same channel is responsible for the activated currents observed in the CFTR-transfected L cells, as a similar channel has been observed in Sf9 insect cells after CFTR infection (14). Further studies are required to determine the single-channel basis of the currents in L cells.

(*iv*) The stably transfected mouse L cells do not require special medium to maintain their Cl^- conductance phenotype, nor do they have a transient life span. They may provide large amounts of CFTR for biochemical or physiological studies.

CFTR expression did not significantly enhance K^+ or Na^+ conductances, indicating that it enhances Cl^- permeability specifically. It has been argued that CFTR may serve to regulate Cl^- channel activity by conferring sensitivity to cAMP or by transporting regulatory factors required for cAMP sensitivity (10, 34). The presence of an endogenous Cl^- conductance in the untransfected L cells appears to support this possibility, but it would require a similar (i.e., highly conserved) pathway in the various CFTR-transfected cells of nonepithelial origin and of different species (refs. 14 and 15 and this study). That a similar cAMP-inducible Cl^- permeability can be detected in the distinct cell types is, therefore, more consistent with an alternate hypothesis that CFTR is itself a Cl^- channel.

A further understanding of the function of CFTR will require more detailed biochemical and physical analyses of the protein. The reproducibility of the CFTR-transfected L cells thus provides the basis of an excellent assay system to dissect the cAMP-inducible Cl^- conductance specific to CF by *in vitro* mutagenesis. These cells could also be useful in screening for other physiological effectors or pharmaceutical agents that may interact with or modify the cAMP-regulated Cl^- conductance associated with CFTR.

We thank T. Jensen, R. Rozmahel, and M. Buchwald. This research was supported by the National Institutes of Health (DK34944; DK41980), the Cystic Fibrosis Foundation, and the Canadian Cystic Fibrosis Foundation. The donation from Mr. Z. Street is gratefully acknowledged. J.K.F. is a Canadian Cystic Fibrosis Foundation Scholar; S.D. is a Canadian Cystic Fibrosis Foundation Fellow; L.-C.T. is a Scientist of the Medical Research Council of Canada.

1. Boat, T., Welsh, M. J. & Beaudet, A. (1989) in *The Metabolic Basis of Inherited Disease*, eds. Scriver, C. R., Beaudet, A. L., Sly, W. S. & Valle, D. (McGraw Hill, New York), 6th Ed., pp. 2649–2680.
2. Rommens, J. M., Iannuzzi, M. C., Kerem, B., Drumm, M. L., Melmer, G., Dean, M., Rozmahel, R., Cole, J. L., Kennedy, D., Hidaka, N., Zsiga, M., Buchwald, M., Riordan, J. R., Tsui, L.-C. & Collins, F. S. (1989) *Science* **245**, 1059–1065.
3. Riordan, J. R., Rommens, J. M., Kerem, B., Alon, N., Rozmahel, R., Grzelczack, Z., Zielenski, J., Lok, S., Plavsic, N., Chou, J.-L., Drumm, M. L., Iannuzzi, M. C., Collins, F. S. & Tsui, L.-C. (1989) *Science* **245**, 1066–1072.
4. Kerem, B., Rommens, J. M., Buchanan, J. A., Markiewicz, D., Cox, T. K., Chakravarti, A., Buchwald, M. & Tsui, L.-C. (1989) *Science* **245**, 1073–1080.
5. Dean, M., White, M. B., Amos, J., Gerrard, B., Stewart, C., Khaw, K.-T. & Leppert, M. (1990) *Cell* **61**, 863–870.
6. Cutting, G. R., Kasch, L. M., Rosenstein, B. J., Zielenski, J., Tsui, L.-C., Kazazian, H. H., Jr., & Antonarakas, S. E. (1990) *Nature (London)* **346**, 366–369.
7. Kerem, B., Zielenski, J., Markiewicz, D., Bozon, D., Gazit, E., Yahav, J., Kennedy, D., Riordan, J. R., Collins, F. S., Rommens, J. M. & Tsui, L.-C. (1990) *Proc. Natl. Acad. Sci. USA* **87**, 8447–8451.
8. White, M. B., Amos, J., Hsu, J. M. C., Gerrard, B., Finn, P. & Dean, M. (1990) *Nature (London)* **344**, 665–667.
9. Zielenski, J., Bozon, D., Kerem, B., Markiewicz, D., Durie, P., Rommens, J. M. & Tsui, L.-C. (1991) *Genomics* **10**, 229–235.
10. Hyde, S. C., Emsley, P., Hartshorn, M. J., Mimmack, M. M., Gileadi, U., Pearce, S. R., Gallagher, M. P., Gill, D. R., Hubbard, R. E. & Higgins, C. F. (1990) *Nature (London)* **346**, 362–365.
11. Gregory, R. J., Cheng, S. H., Rich, D. P., Marshall, J., Paul, S., Hehir, K., Ostedgaard, L., Klinger, K. W., Welsh, M. J. & Smith, A. E. (1990) *Nature (London)* **347**, 382–386.
12. Drumm, M. L., Pope, H. A., Cliff, W. H., Rommens, J. M., Marvin, S. A., Tsui, L.-C., Collins, F. S., Frizzell, R. A. & Wilson, J. M. (1990) *Cell* **62**, 1227–1233.
13. Rich, D. P., Anderson, M. P., Gregory, R. J., Cheng, S. H., Paul, S., Jefferson, D. M., McCann, J. D., Klinger, K. W., Smith, A. E. & Welsh, M. J. (1990) *Nature (London)* **347**, 358–363.
14. Kartner, N., Jensen, T. J., Naismith, A. L., Sun, S., Ackerley, C. A., Reyes, E. F., Tsui, L.-C., Rommens, J. M., Bear, C. E. & Riordan, J. R. (1991) *Cell* **64**, 681-691.
15. Anderson, M. P., Rich, D. P., Gregory, R. J., Smith, A. E. & Welsh, M. J. (1991) *Science* **251**, 679–682.
16. Meakin, S. O., Du, R. P., Tsui, L.-C. & Breitman, M. L. (1987) *Mol. Cell. Biol.* **7**, 2671–2679.
17. Karin, M. & Richards, R. I. (1982) *Nature (London)* **299**, 797–802.
18. Sambrook, J., Fritsch, E. F. & Maniatis, T. (1989) *Molecular Cloning: A Laboratory Manual* (Cold Spring Harbor Lab., Cold Spring Harbor, NY), 2nd Ed.
19. Higuchi, R., Krummel, B. & Saiki, R. K. (1988) *Nucleic Acids Res.* **16**, 7351–7363.
20. Ho, S. N., Hunt, H. D., Horton, R. M., Pullen, J. K. & Pease, L. R. (1989) *Gene* **77**, 51–59.
21. Miller, S. A., Dykes, D. D. & Polesky, H. F. (1988) *Nucleic Acids Res.* **16**, 1215.
22. MacDonald, R. J., Swift, G. H., Przybyla, A. E. & Chirgwin, J. M. (1987) *Methods Enzymol.* **152**, 219–227.
23. Laemmli, U. K. (1970) *Nature (London)* **227**, 680–685.
24. Towbin, H., Staehelin, T. & Gordon, J. (1979) *Proc. Natl. Acad. Sci. USA* **76**, 4350–4354.
25. Foskett, J. K. (1988) *Am. J. Physiol.* **255**, C566–C571.
26. Foskett, J. K. & Melvin, J. E. (1989) *Science* **244**, 1582–1585.
27. Foskett, J. K. (1990) *Am. J. Physiol.* **259**, C998–C1004.
28. Hamill, O. P., Marty, A., Neher, E., Sakmann, B. & Sigworth, F. J. (1981) *Pflügers Arch.* **391**, 85–100.
29. Cheng, S. H., Gregory, R. J., Marshall, J., Paul, S., Souza, D. W., White, G. A., O'Riordan, C. R. & Smith, A. E. (1990) *Cell* **63**, 827–834.
30. Illsley, N. P. & Verkman, A. S. (1987) *Biochemistry* **26**, 1215–1219.
31. Cliff, W. H. & Frizzell, R. A. (1990) *Proc. Natl. Acad. Sci. USA* **87**, 4956–4960.
32. Tabcharani, J. A., Low, W., Elie, D. & Hanrahan, J. W. (1990) *FEBS Lett.* **270**, 157–164.
33. Gray, M. A., Pollard, C. E., Harris, A., Coleman, L., Greenwell, J. R. & Argent, B. E. (1990) *Am. J. Physiol.* **259**, C752–C761.
34. Ringe, D. & Petsko, G. A. (1990) *Nature (London)* **346**, 312–313.